DPMJET-III and p-p data from LHC

J.Ranft, Siegen University, Germany

Trento 2010

Comparison of DPMJET-III with p-p collision results from the LHC

Remarks:

The LHC experiments replace the PYTHIA code used by PHOJET (DPMJET-III) by a newer version.

This has the effect, (if they compare their data to PHOJET) that the PHOJET multiplicity is lowered against the original PHOJET

Ralph Engel is working on a new PHOJET version, which probably will not be available before the end of the year

(1) DPMJET–III Status and problems.

h–h collisions: PHOJET in DPMJET–III

R.Engel Z.Phys. C66, 203, (1995)

R.Engel and J.Ranft Phys. Rev. D54, 4244, (1996)

h–A, A–A collisions: DPMJET–III

S.Roesler, R.Engel and J.Ranft Proc. of Monte Carlo 2000 (Lisboa), Springer, p.1033 (2000)

Dpmjet-III is using Phojet1.12 .

Using Phojet for calculating hadron-hadron interactions and hadronic interactions involving photons, Dpmjet-III allows also the simulation of photoproduction off nuclei.

The construction of the PHOJET multichain model

The (soft) Born cross section of the supercritical pomeron has the form

$$\sigma_s = g^2 s^{\alpha(0)-1}. \qquad (1)$$

The supercritical pomeron has $\alpha(0) > 1.$, therefore (1) clearly violates unitarity.

According to the Froissart bound the cross section asymptotically should not rise faster than $(\log s)^2$.

If we start to construct the full model, which is unitarized, we should introduce some more input Born cross sections.

The hard cross section, which we calculate according to the QCD improved parton model

$$\sigma^{\text{hard}}(s, p_\perp^{\text{cutoff}}) = \int dx_1 dx_2 d\hat{t} \sum_{i,j,k,l} \frac{1}{1+\delta_{k,l}}$$

$$f_{a,i}(x_1, Q^2) f_{b,j}(x_2, Q^2) \frac{d\sigma^{\text{QCD}}_{i,j\to k,l}(\hat{s}, \hat{t})}{d\hat{t}} \Theta(p_\perp - p_\perp^{\text{cutoff}}), \qquad (2)$$

where $f_{a,i}(x_1, Q^2)$ is the distribution of the parton i in a.

We introduce furthermore the cross sections for high–mass single and double diffraction σ_D and for high–mass central diffraction σ_C according to the standard expressions.

The amplitudes corresponding to the one-pomeron exchange are unitarized applying a eikonal formalism

In impact parameter representation, the eikonalized scattering amplitude has the structure

$$a(s,B) = \frac{i}{2}\left(\frac{e^2}{f_{q\bar{q}}^2}\right)^2 \left(1 - e^{-\chi(s,B)}\right) \tag{3}$$

with the eikonal function

$$\chi(s,B) = \chi_S(s,B) + \chi_H(s,B) + \chi_D(s,B) + \chi_C(s,B). \tag{4}$$

Here, $\chi_i(s,B)$ denotes the contributions from the different Born graphs: (S) soft part of the pomeron and reggeon, (H) hard part of the pomeron (D) triple- and loop-pomeron, (C) double-pomeron graphs.

The eikonals $\chi_i(s,B)$ are defined as follows

$$\chi_i(s,B) = \frac{\sigma_i(s)}{8\pi b_i}\exp[-\frac{B^2}{4b_i}]. \tag{5}$$

The free parameters are fixed by a global fit to proton-proton cross sections and elastic slope parameters.

Once the free parameters are determined, the probabilities for the different final state configurations are calculated from the discontinuity of the elastic scattering amplitude (optical theorem).

The total discontinuity can be expressed as a sum of graphs with k_c soft pomeron cuts, l_c hard pomeron cuts, m_c triple- or loop-pomeron cuts, and n_c double-pomeron cuts by applying the Abramovski-Gribov-Kancheli cutting rules .

In impact parameter space one gets for the inelastic cross section

$$\sigma(k_c, l_c, m_c, n_c, s, B) = \frac{(2\chi_S)^{k_c}}{k_c!}\frac{(2\chi_H)^{l_c}}{l_c!}\frac{(2\chi_D)^{m_c}}{m_c!}\frac{(2\chi_C)^{n_c}}{n_c!}\exp[-2\chi(s, B)] \tag{6}$$

with

$$\int d^2B \sum_{k_c+l_c+m_c+n_c=1}^{\infty} \sigma(k_c, l_c, m_c, n_c, s, B) \approx \sigma_{\text{tot}} \qquad (7)$$

where σ_{tot} denote the total cross section

In the Monte Carlo realization of the model, the different final state configurations are sampled from Eq. (6).

For pomeron cuts involving a hard scattering, the complete parton kinematics and flavors/colours are sampled according to the Parton Model.

For pomeron cuts without hard large momentum transfer, the partonic interpretation of the Dual Parton Model is used: mesons

are split into a quark-antiquark pair whereas baryons are approximated by a quark-diquark pair.

The longitudinal momentum fractions of the partons are given by Regge asymptotics . We give it here for an event with n_s soft and $n_h (n_h \geq 1)$ hard cut pomerons, sea–quarks are used at the chain ends if we have more than one soft pomeron.

$$\rho(x_1, ..., x_{2n_s}, ..., x_{2n_s+2+n_h}) \sim \frac{1}{\sqrt{x_1}} \left(\prod_{i=3}^{2n_s+2} \frac{1}{x_i} \right) x_2^{1.5} \prod_{i=2n_s+3}^{2n_s+2+n_h} g(x_i, Q_i) \delta\left(1 - \sum_{i=1}^{2n_s+2+n_h} x_i\right). \quad (8)$$

The distributions $g(x_i, Q_i)$ are the distribution functions of the partons engaged in the hard scattering. The momentum fractions of the constituents at the ends of the different chains are sampled from this exclusive parton distribution,

After all this we we have all chains defined and we continue with hadronizing all multiple chains using the Lund code JETSET (PYTHIA).

Now we are able to compare the multichain model with particle production data.

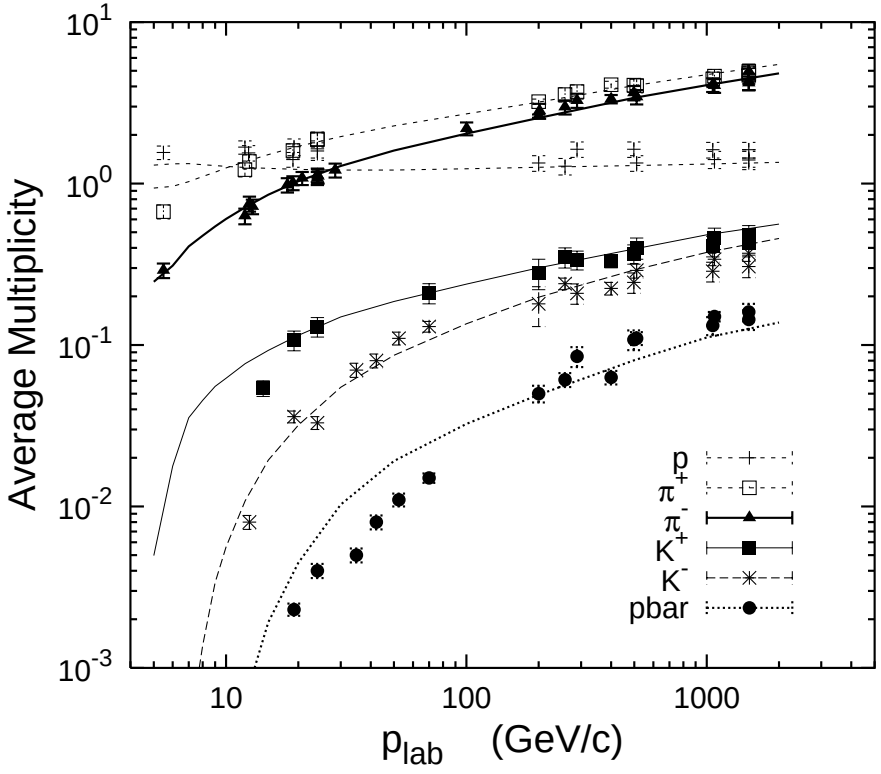

Average particle multiplicity proton-proton interactions. Phojet results (curves) are compared to experimental data (symbols).

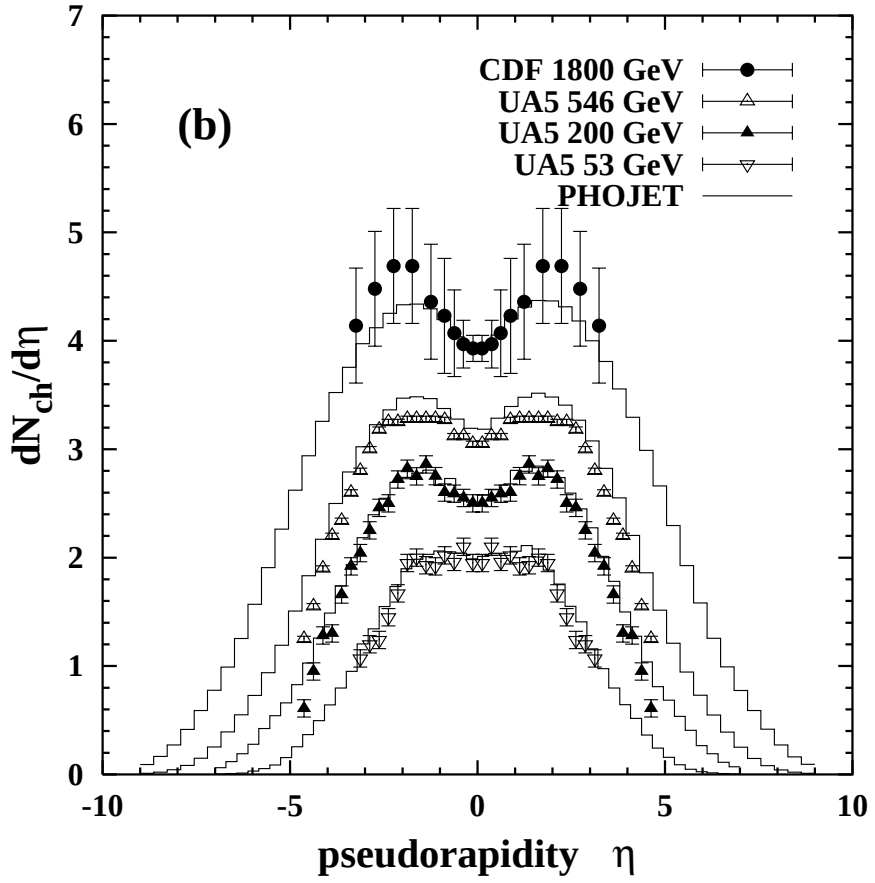

Energy-dependence of charged particle pseudorapidity density in $p\bar{p}$ collisions. phojet is compared to data from different colliders

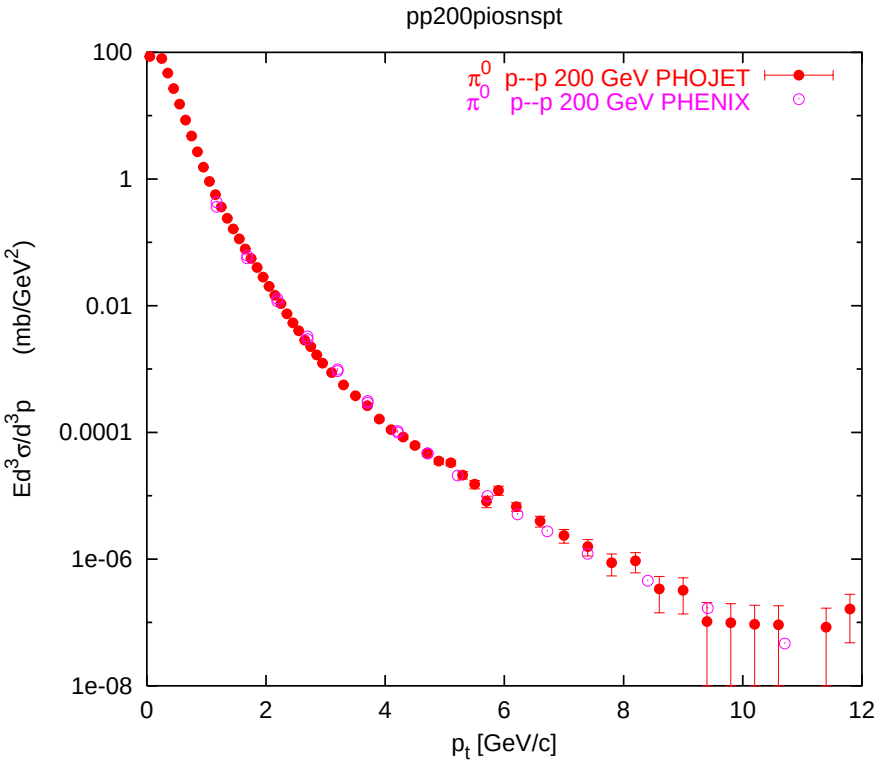

Transverse momentum distribution as measured in p–p collisions at $\sqrt{s} = 200$ GeV by the PHENIX collaboration at RHIC compared to the calculation by phojet

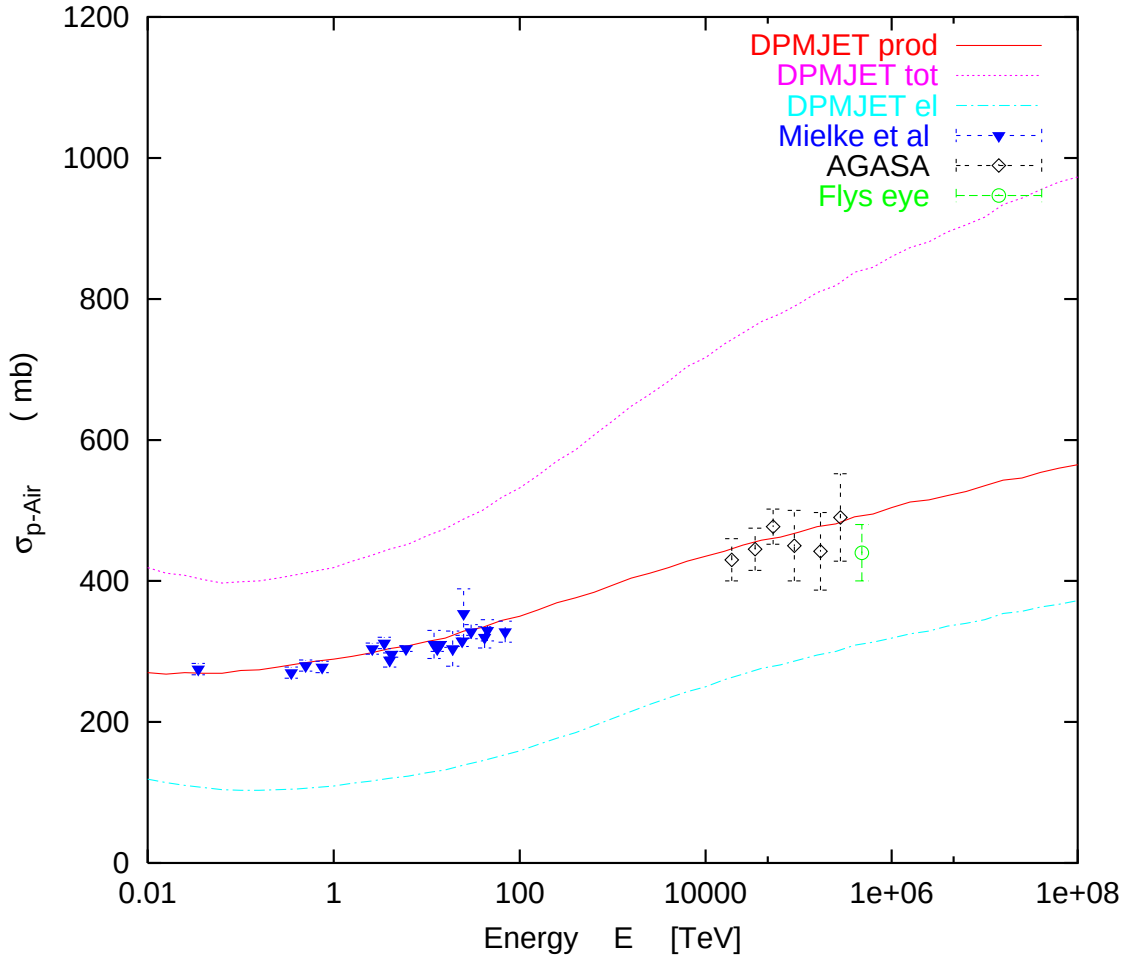

The inelastic cross section σ_{p-Air} calculated by Dpmjet as function of the laboratory energy E compared to experimental data collected by Mielke et al. and from AGASA and Fly's eye.

(4) RHIC data and the DPM–models (DPMJET–III)

We first present some comparisons, where DPMJET-III is used in its pre–RHIC form:

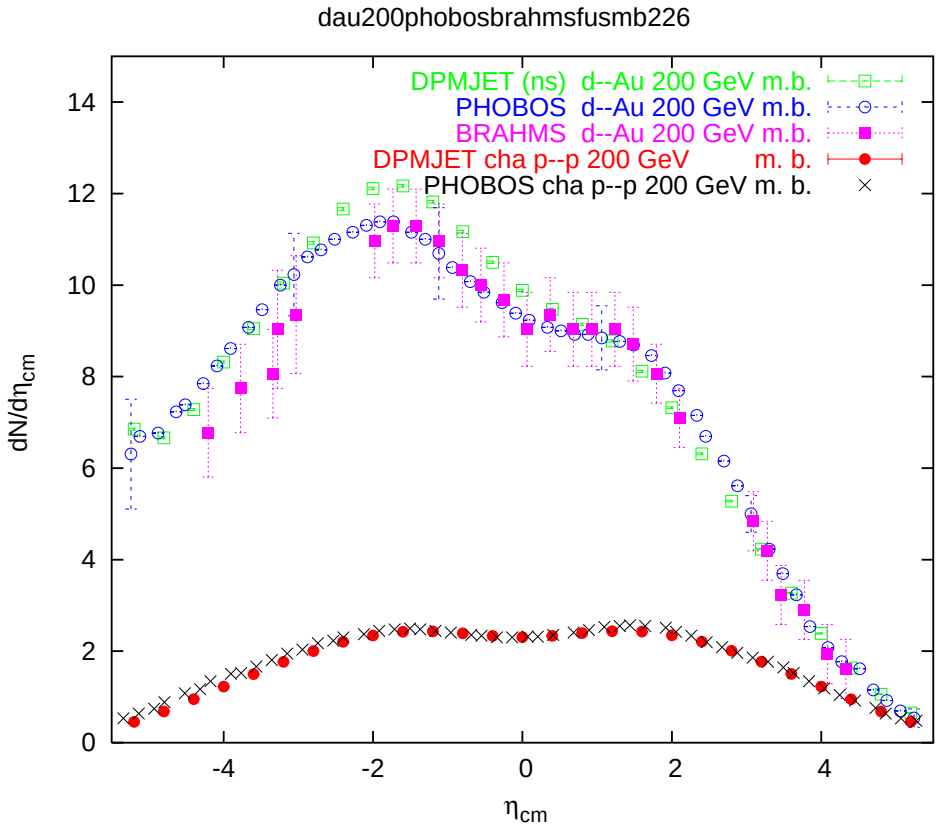

Pseudorapidity distribution of charged hadrons produced in minimum bias $\sqrt{s} = 200$ GeV d–Au and p–p collisions. The results of Dpmjet are compared to experimental data from the BRAHMS–Collaboration and the PHOBOS–Collaboration. At some pseudorapidity values the systematic PHOBOS–errors are given.

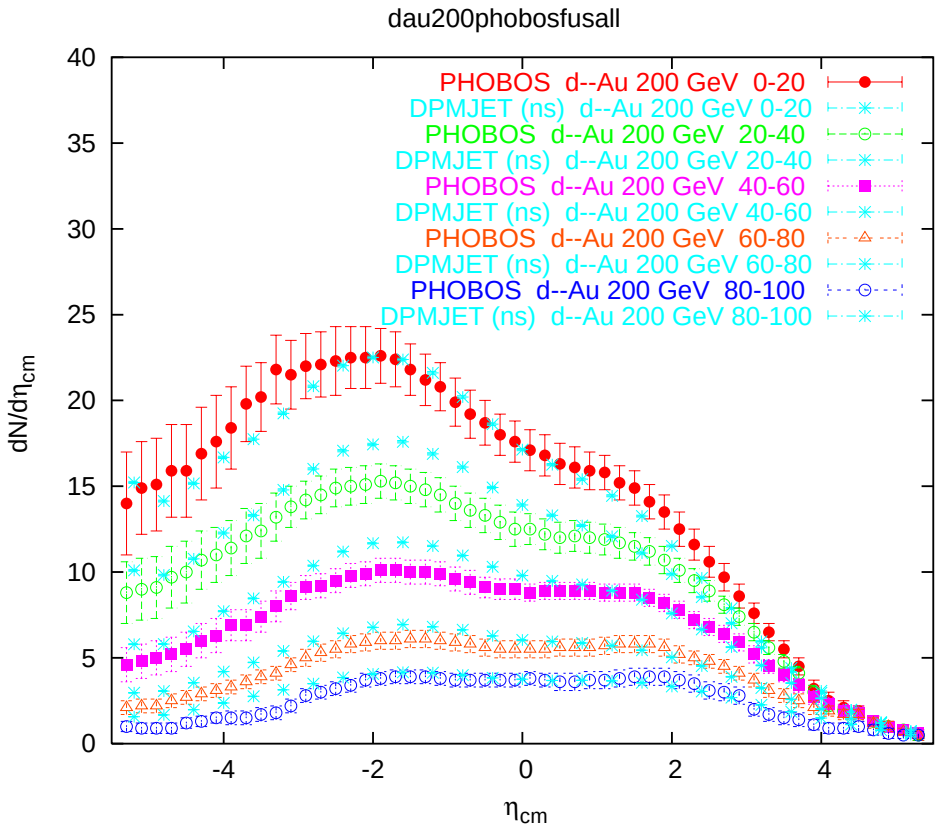

Pseudorapidity distribution of charged hadrons produced in non-single-diffractive (ns) $\sqrt{s} =$ 200 GeV d–Au collisions with different centralities. The results of Dpmjet are compared to preliminary data from the PHOBOS–Collaboration.

Percolation and chain fusion

With our interest in Cosmic Ray particle production we are most interested in p–p collisions and collisions involving light nuclei.

(i)Average multiplcities and pseudorapidity distributions in collisions involving nuclei at different centralities.

(ii)Particle production ratios at different centralities.

(iii)$p_\perp$ and $E_\perp$ distributions of identified hadrons and R_{AA} ratios

$$R_{AA} = \frac{\frac{d^2N^{A-A}}{dp_\perp d\eta}}{N_{binary}^{A-A}\frac{d^2N^{N-N}}{dp_\perp d\eta}} \tag{9}$$

Percolation and chain fusion

The groups at Lisboa (Dias de Deus et al) and Santiago de Compostela (Pajares, Braun) were the first to point out, that the multiplicities measured at RHIC are significantly lower than predicted by conventional multi–string models.

A new mechanism is needed to lower the multiplicity in situations with a very high density of produced hadrons like in central nucleus–nucleus collisions.

The percolation and fusion of strings, the building blocks of the multi–string models is one such mechanism.

The result of chain percolation expressed in the most simple way is a decrease of the multiplicity and an increase of the average transverse momenta.

Using the original Dpmjet–III with enhanced baryon stopping and a centrality of 0 to 5 % we compare to some multiplicities measured in Au–Au collisions at RHIC.

At $\sqrt{(s)} = 130$ GeV Dpmjet–III gives $N_{ch} = 6031$, BRAHMS finds $N_{ch} = 3860 \pm 300$.

Again at $\sqrt{(s)} = 130$ GeV Dpmjet–III gives a plateau$dN_{ch}/d\eta|_{\eta=0} = 968$, BRAHMS finds $dN_{ch}/d\eta|_{\eta=0} = 553 \pm 36$, PHOBOS finds $dN_{ch}/d\eta|_{\eta=0} = 613 \pm 24$ and PHENIX finds $dN_{ch}/d\eta|_{\eta=0} = 622 \pm 41$.

There is indeed a new mechanism needed to reduce N_{ch} and $dN_{ch}/d\eta|_{\eta=0}$ in situations with a produced very dense hadronic system.

Percolation of hadronic strings in Dpmjet–III

We consider only the percolation and fusion of soft chains (transverse momenta of both chain ends below a cut–off $p_{\perp}^{fusion} = 2$ GeV/c

The condition of percolation is, that the chains overlap in transverse space.

We calculate the transverse distance of the chains L and K R_{L-K} and allow fusion of the chains for $R_{L-K} \leq R^{fusion} = 0.75$ fm.

The chains in Dpmjet are fragmented using the Lund code

Only the fragmentation of color triplet–antitriplet chains is available in Jetset, however fusing two arbitrary chains could result in chains with other colors.

Therefore, we select only chains for fusion, which again result in triplet–antitriplet chains.

(i)A $q_1 - \bar{q}_2$ plus a $q_3 - \bar{q}_4$ chain become a $q_1 q_3 - \bar{q}_2 \bar{q}_4$ chain.

(ii)A $q_1 - q_2 q_3$ plus a $q_4 - \bar{q}_2$ chain become a $q_1 q_4 - q_3$ chain.

(iii)A $q_3 - q_1 q_2$ plus a $q_4 - \bar{q}_1$ plus a $\bar{q}_3 - q_5$ chain become a $q_4 - q_2 q_5$ chain.

(iv)A $q_4 - \bar{q}_1$ plus a $q_5 - \bar{q}_3$ plus a $\bar{q}_5 - q_1$ chain become a $q_4 - \bar{q}_3$ chain.

The expected results of these transformations are a decrease of the number of chains.

Even when the fused chains have a higher energy than the original chains, the result will be a decrease of the hadron multiplicity $N_{hadrons}$.

In reaction (i) we observe new diquark and anti–diquark chain ends. In the fragmentation of these chains we expect baryon–antibaryon production anywhere in the rapidity region of the collision.

Therefore, (i) helps to shift the antibaryon to baryon ratio of the model into the direction as observed in the RHIC experiments.

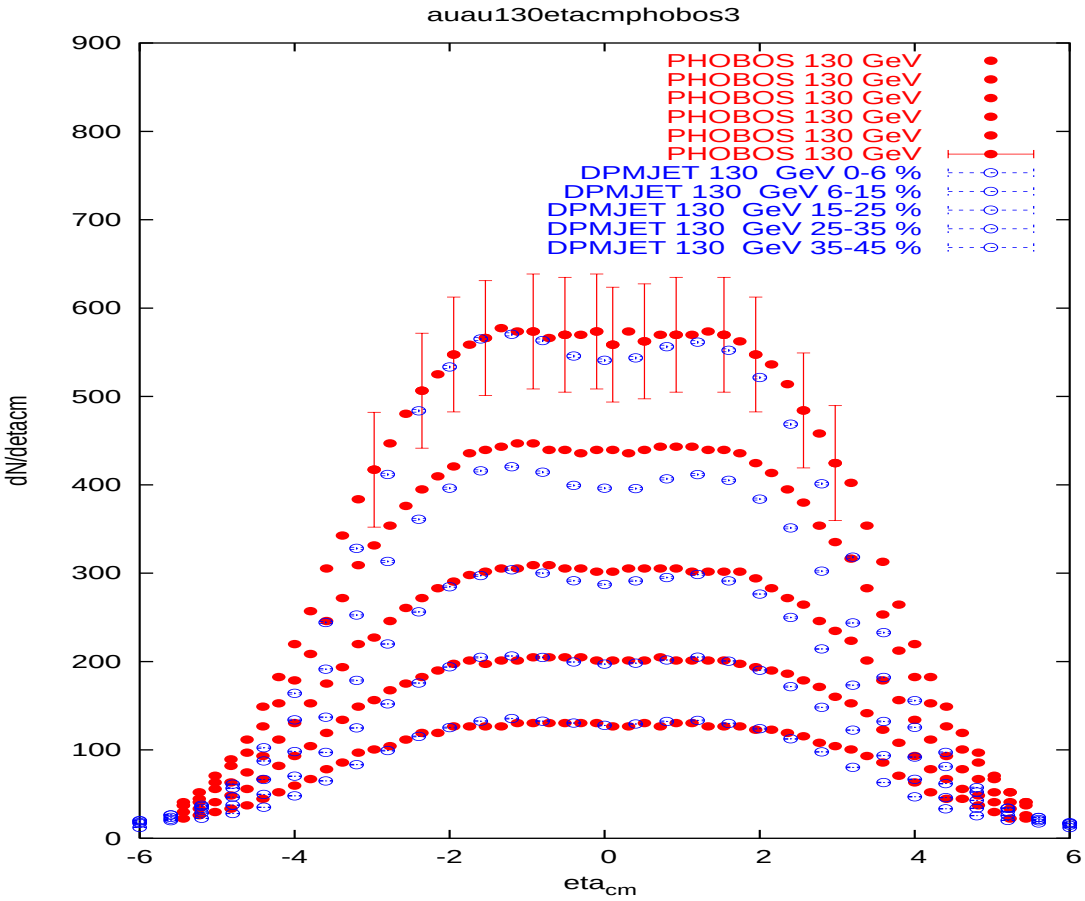

Pseudorapidity distributions of charged hadrons in Au–Au collisions at $\sqrt{(s)}$= 130 GeV for centralities 0–5 % up to 40–50 %. The points with rather small error bars are from the Dpmjet–III Monte Carlo with chain fusion as described in the text. The data points are from the PHOBOS Collaboration

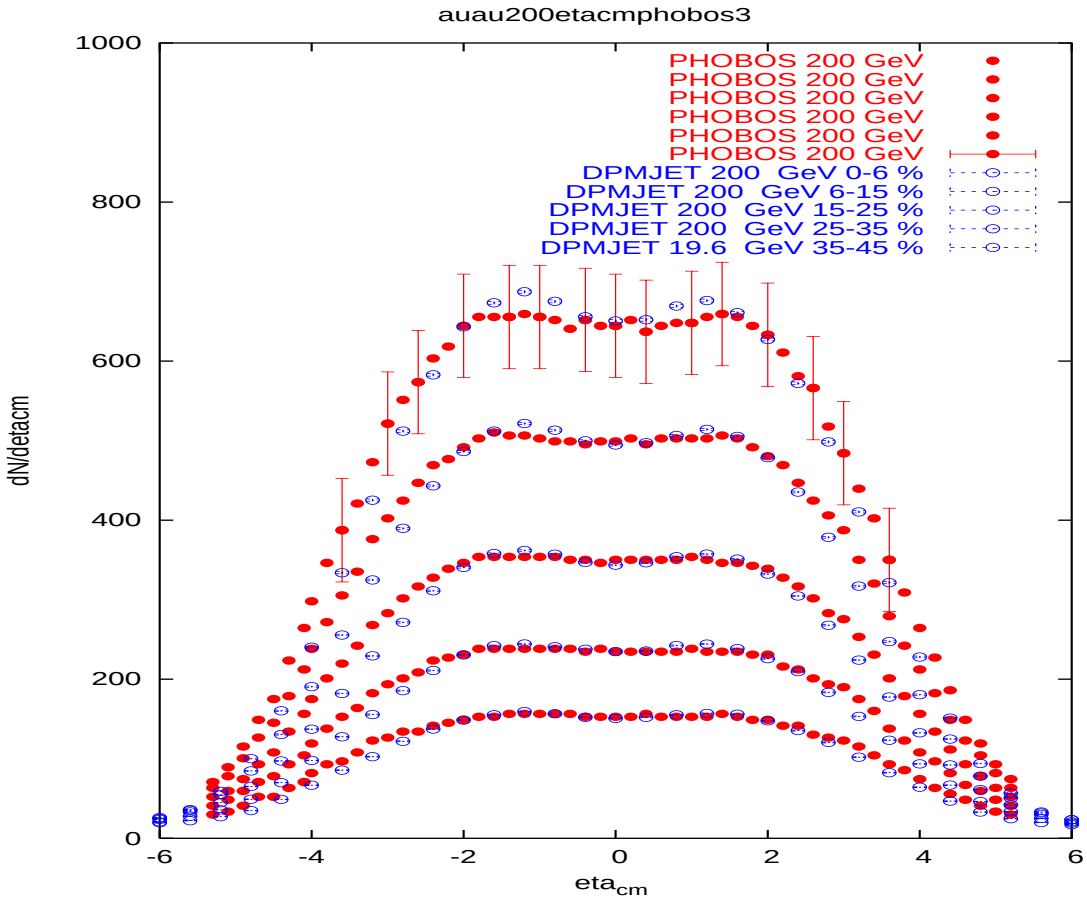

Pseudorapidity distributions of charged hadrons in Au–Au collisions at $\sqrt{(s)}$= 200 GeV for centralities 0–5 % up to 40–50 %. The points with rather small error bars are from the Dpmjet–III Monte Carlo with chain fusion as described in the text. The data points are from the PHOBOS Collaboration

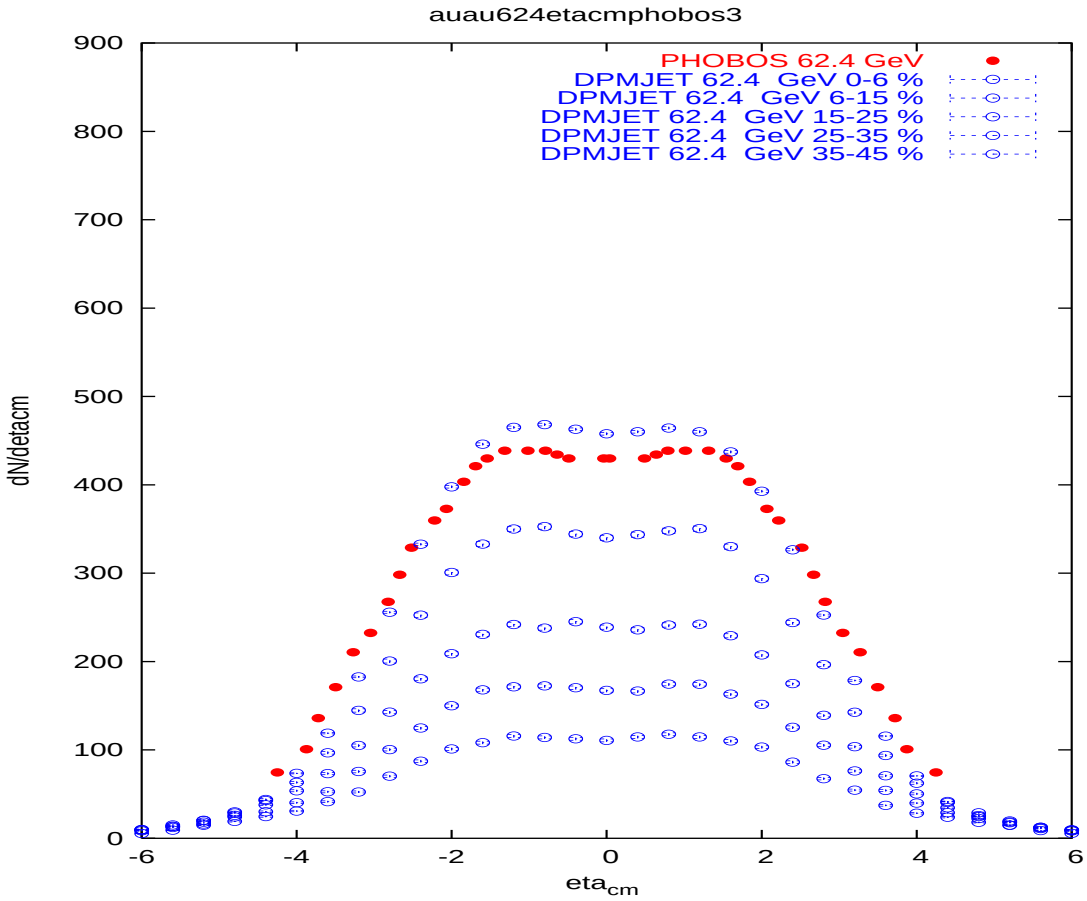

Pseudorapidity distributions of charged hadrons in Au–Au collisions at $\sqrt{(s)}$= 62.4 GeV for centralities 0–5 % up to 40–50 %. The points with rather small error bars are from the Dpmjet–III Monte Carlo with chain fusion as described in the text. The data points are from the PHOBOS Collaboration

We apply DPMJET–III with chain fusion to central Pb–Pb collisions

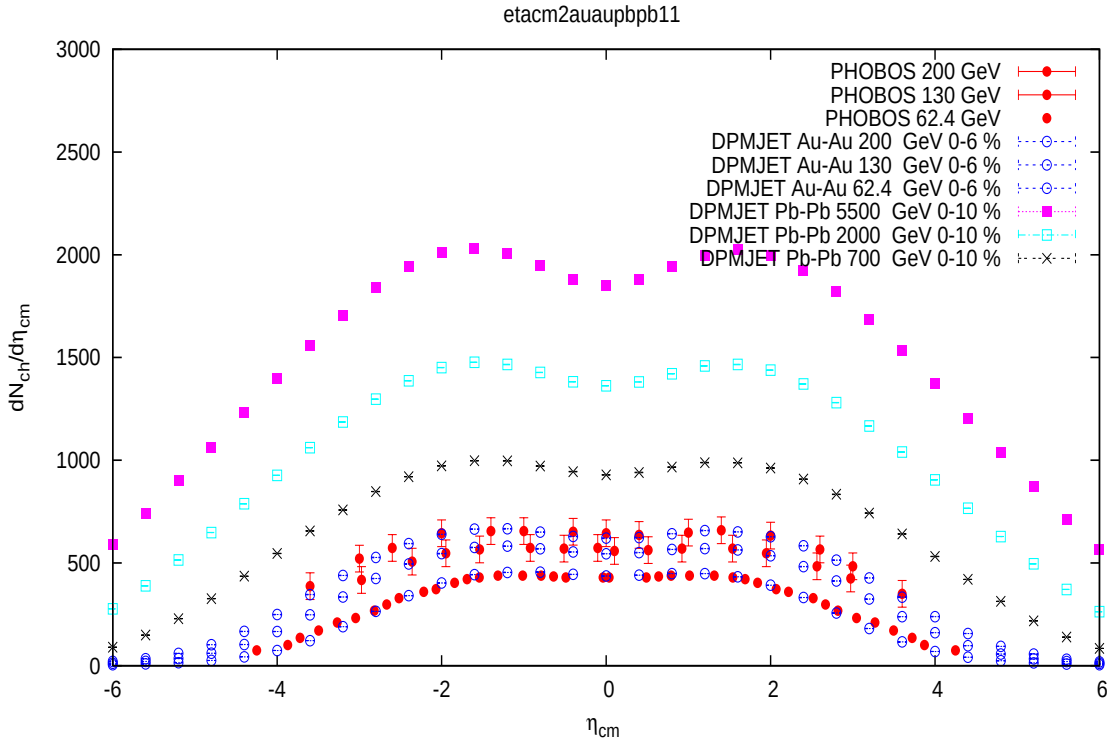

Pseudorapidity distributions of charged hadrons in Au–Au collisions at $\sqrt{(s)}$= 200, 130 and 62.4 GeV for centralities 0–6 % and for Pb–Pb collisions at 5500, 2000 and 700 GeV for centralities 0–10 %. The data points are from the PHOBOS Collaboration

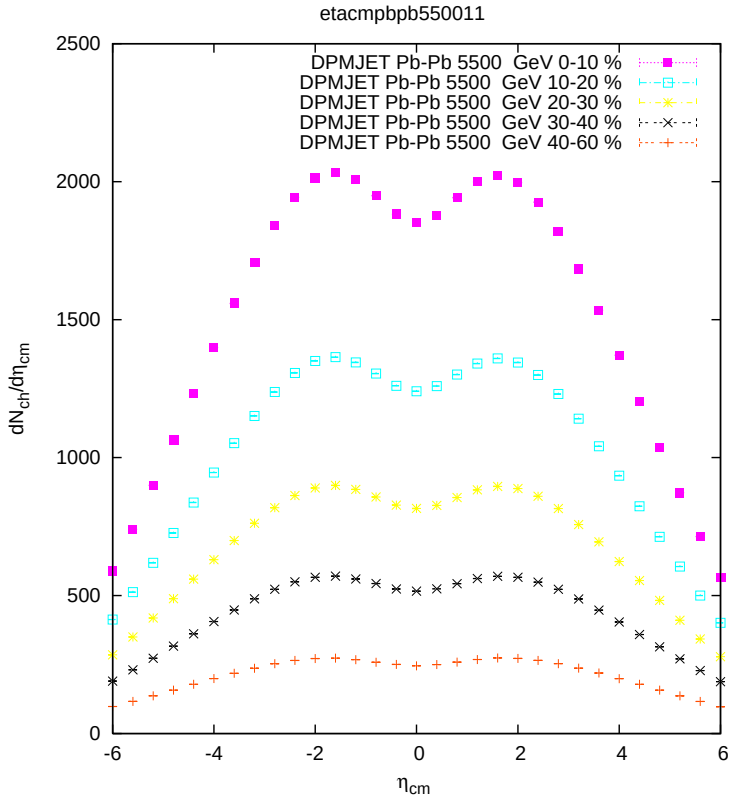
etacmpbpb550011
DPMJET Pb-Pb 5500 GeV 0-10 %
DPMJET Pb-Pb 5500 GeV 10-20 %
DPMJET Pb-Pb 5500 GeV 20-30 %
DPMJET Pb-Pb 5500 GeV 30-40 %
DPMJET Pb-Pb 5500 GeV 40-60 %
dN_ch/dη_cm
η_cm
0
500
1000
1500
2000
2500
-6
-4
-2
0
2
4
6

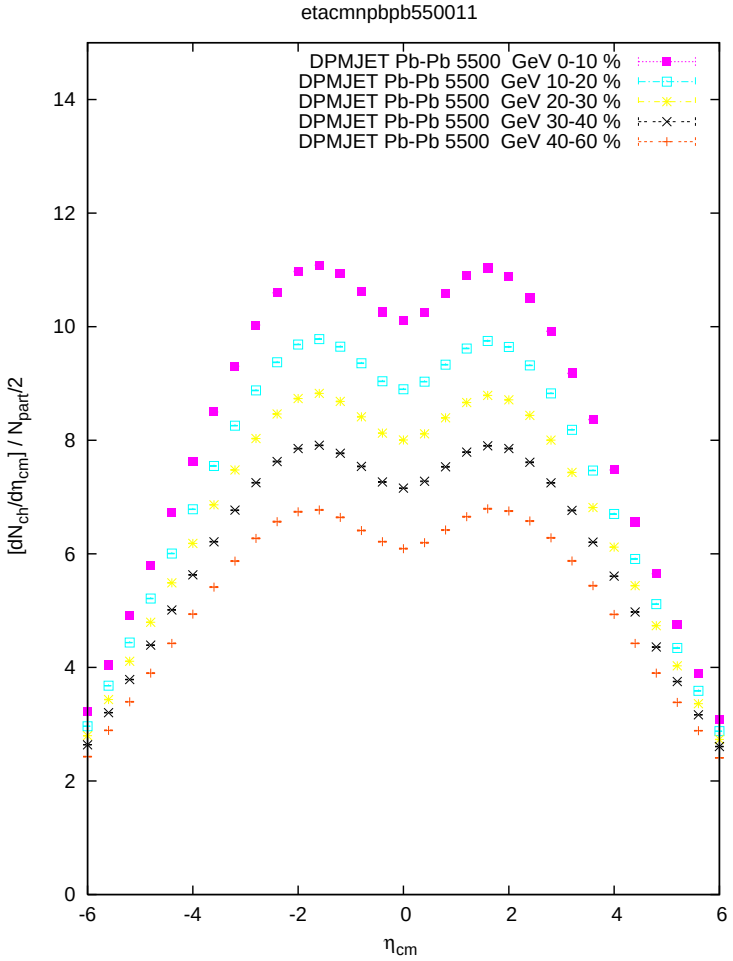
etacmnpbpb550011
DPMJET Pb-Pb 5500 GeV 0-10 %
DPMJET Pb-Pb 5500 GeV 10-20 %
DPMJET Pb-Pb 5500 GeV 20-30 %
DPMJET Pb-Pb 5500 GeV 30-40 %
DPMJET Pb-Pb 5500 GeV 40-60 %
[dN_ch/dη_cm] / N_part/2
η_cm
0
2
4
6
8
10
12
14
-6
-4
-2
0
2
4
6

Collision scaling in h–A collisions

Several RHIC experiments (for instance PHENIX) find in d-Au collisions at large $p_\perp$ a nearly perfect collision scaling for π^0 production. Collision scaling means $R_{AA} \approx 1.0$.

The R_{AA} ratios are defined as follows:

$$R_{AA} = \frac{\frac{d^2}{dp_\perp d\eta} N^{A-A}}{N^{A-A}_{binary} \cdot \frac{d^2}{dp_\perp d\eta} N^{N-N}} \tag{10}$$

Here N^{A-A}_{binary} is the number of binary Glauber collisions in the nucleus–nucleus collision A–A.

Dpmjet–III in its original form gave for π^0 production in d+Au collisions strong deviations from collision scaling ($R_{AA} \approx 0.5$ at large $p_\perp$).

The reason for this was in the iteration procedure to sample the multiple collisions in Dpmjet:

some soft and hard collisions were rejected by this iteration procedure.

Using a reordered iteration procedure it was possible to obtain a nearly perfect collision scaling, see the next Fig.

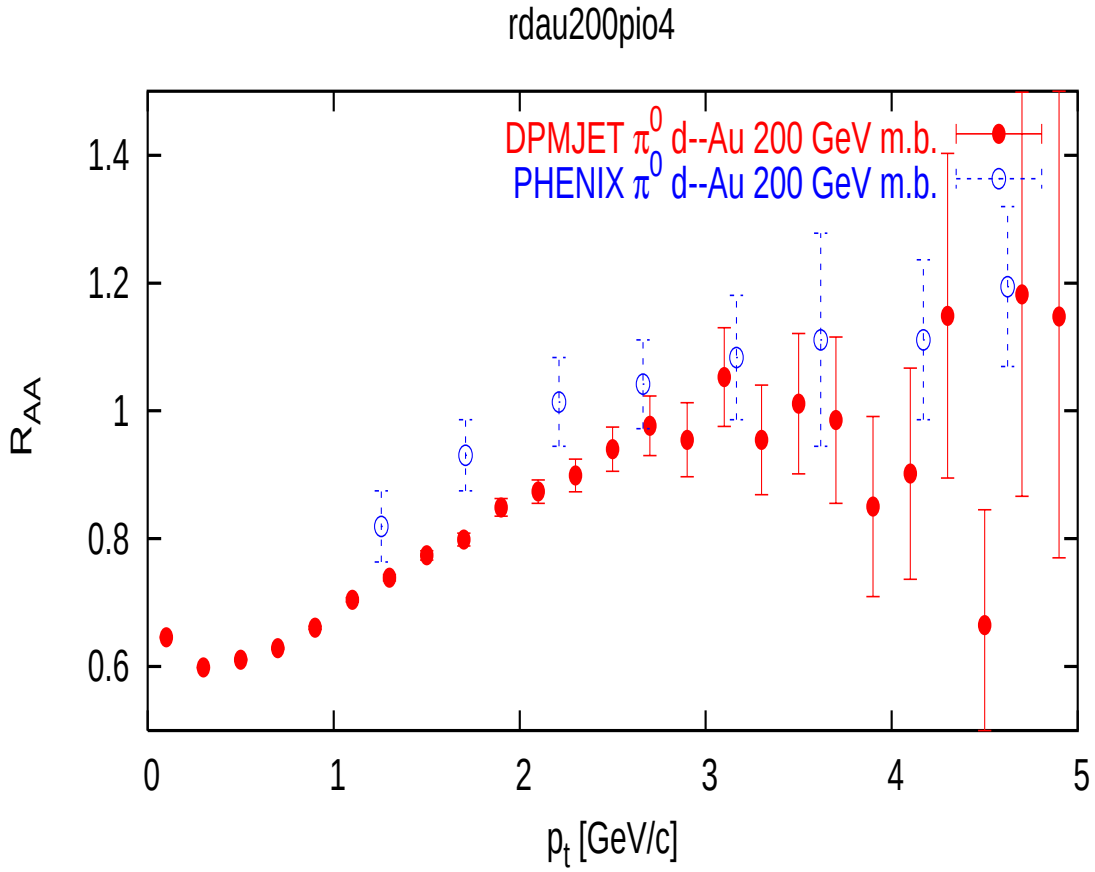

R_{AA} ratio of π^0–mesons produced in $\sqrt{s} = 200$ GeV d–Au collisions. The results of the modified Dpmjet are compared to experimental data from the PHENIX–Collaboration.

LHC hadron production data can be found in:

CMS

HEP-ex 1002.0621: NSD plateau and pt distributions at 900 and 2360 GeV

HEP-ex 1005.3299: NSD plateau and pt distributions at 7000 GeV

HEP-ex 1006.0948: Inclusive distributions at 0.9 and 2.36 TeV

HEP-ex 1006.2083: Underlying event

HEP-ex 1006.4010: Status

HEP-ex 1009.4122: Long range near side angular correlations. This paper is not yet analyzed here. (elliptical flow?!)

ALICE

HEP-ex 1004.3514: Multiplicity distributions at 7000 GeV

HEP-ex 1004.3034: Multiplicity distributions at 2360 GeV and 900 GeV

hep-ex 1006.5432: nsd central p-bar to p ratios at 900 and 7000 GeV

hep-ex 1007.0516: Bose Einstein correlations at 900 GeV

hep-ex 1007.0719: pt distributions at 900 GeV

ATLAS

hep-ex 1003.3124: plateau at 900 GeV

hep-ex 1005.4569: simulation infrastructure

hep-ex 1005.5254: performance of detector

I use DPMJET (with PYTHIA parameters I use most of the time)

PYTHIA is used without private changes in the routine pyptdi, this PYTHIA file I call pythia6115orig.f.

In addition I have at 900 GeV COLLSCA 0.08, at 2360 GeV COLLSCA 0.2 and at 7000 GeV COLLSCA 0.3

The PARJ(41) and PARJ(42) parameters become energy dependent:

E-cm .GT. 4TeV PARJ(41)=0.3, PARJ(42)=0.6

E-CM .LT. 4TeV PARJ(41)=0.3-(4000.-E-cm)*0.15/3100.

PARJ(42)=0.6+(4000.-E-cm)*0.15/3100.

First the nsd-plateau measured by CMS for —eta-cm— smaller then 2.4, we compare for eta-cm = 0. We compare in addition with data at 200 and 540 GeV.

	200 GeV	540 GeV	900 GeV	2360 GeV	7000 GeV
Exp.	2.40	3.34	3.48+-0.15	4.47+-0.20	5.78+-0.24
DPM	2.38	2.99	3.55	4.54	5.83

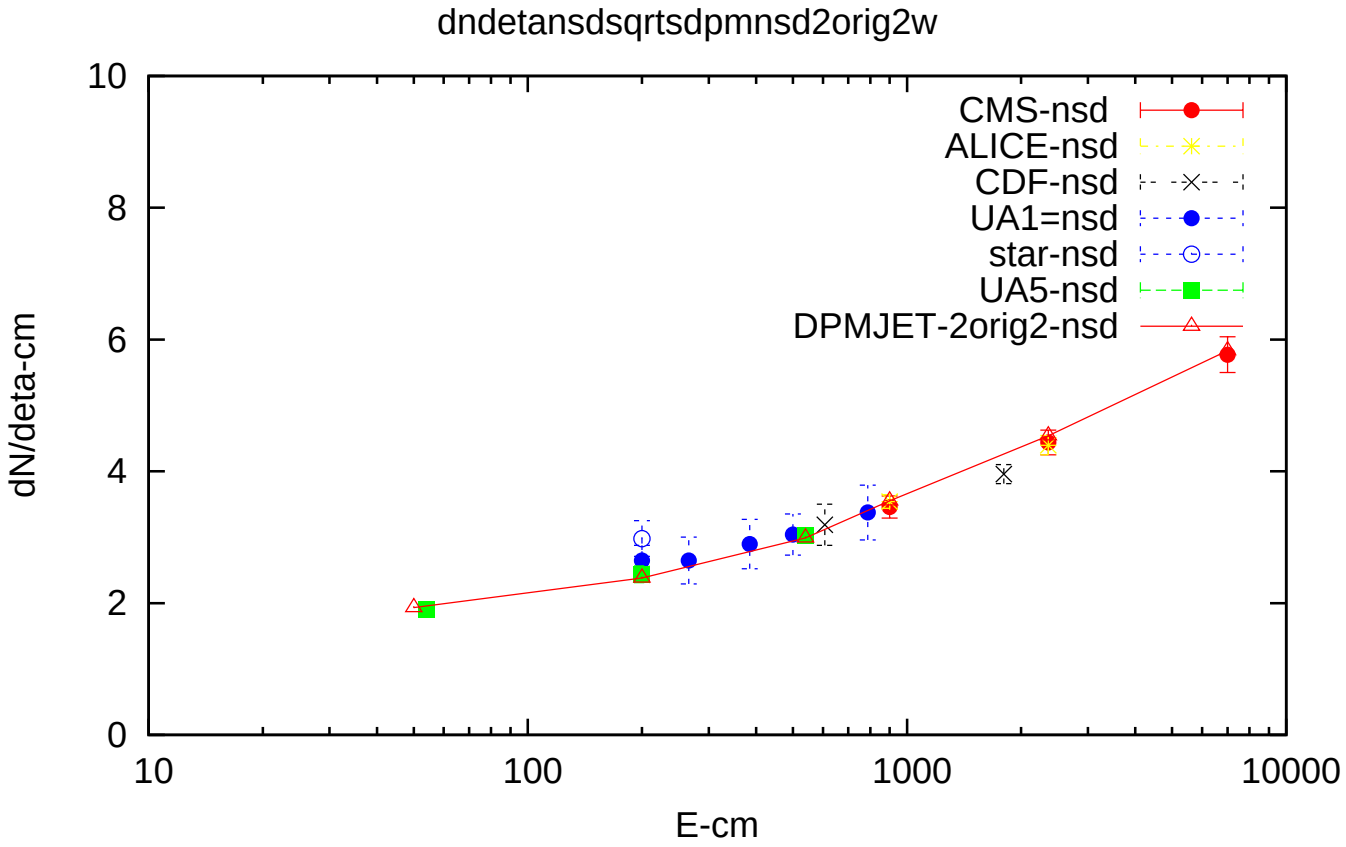
dndetansdsqrtsdpmnsd2orig2w
dN/deta-cm
E-cm
0
2
4
6
8
10
10
100
1000
10000
CMS-nsd
ALICE-nsd
CDF-nsd
UA1=nsd
star-nsd
UA5-nsd
DPMJET-2orig2-nsd

We Compare the pseudorapidity distributions with the CMS data

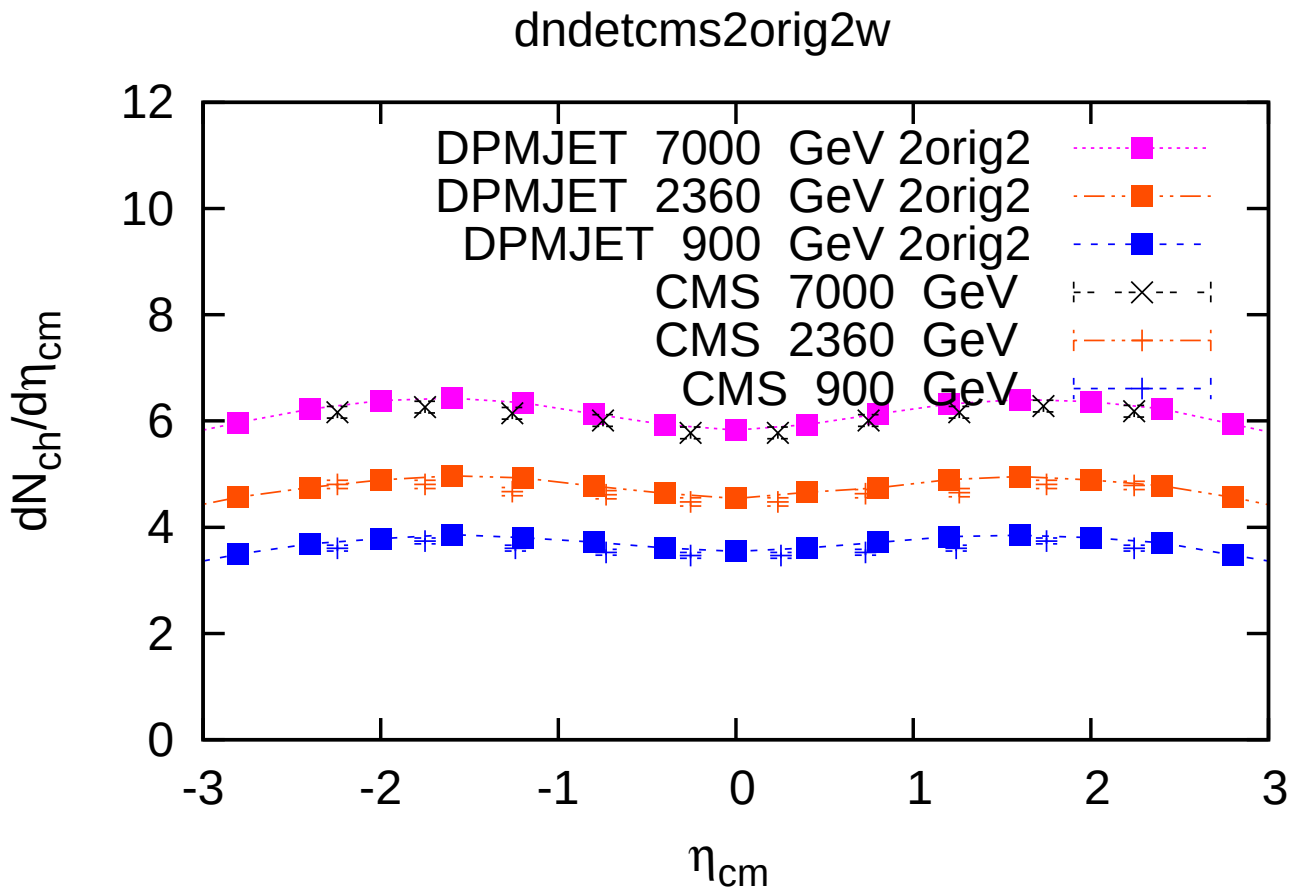

Second nsd average pt values, again we also compare at 200 and 540 GeV.

	200 GeV	540 GeV	900 GeV	2360 GeV	7000 GeV
Exp.	0.395	0.425	0.46+-0.02	0.50+-0.02	0.545+-0.02
DPM	0.411	0.447	0.464	0.494	0.530

ALICE measured central nsd p-bar/p ratios at 900 and 7000 GeV

	900 GeV	7000 GeV
ALICE	0.957+-0.015	0.991+-0.015
DPMJET	0.976+-0.016	1.016+-0.016

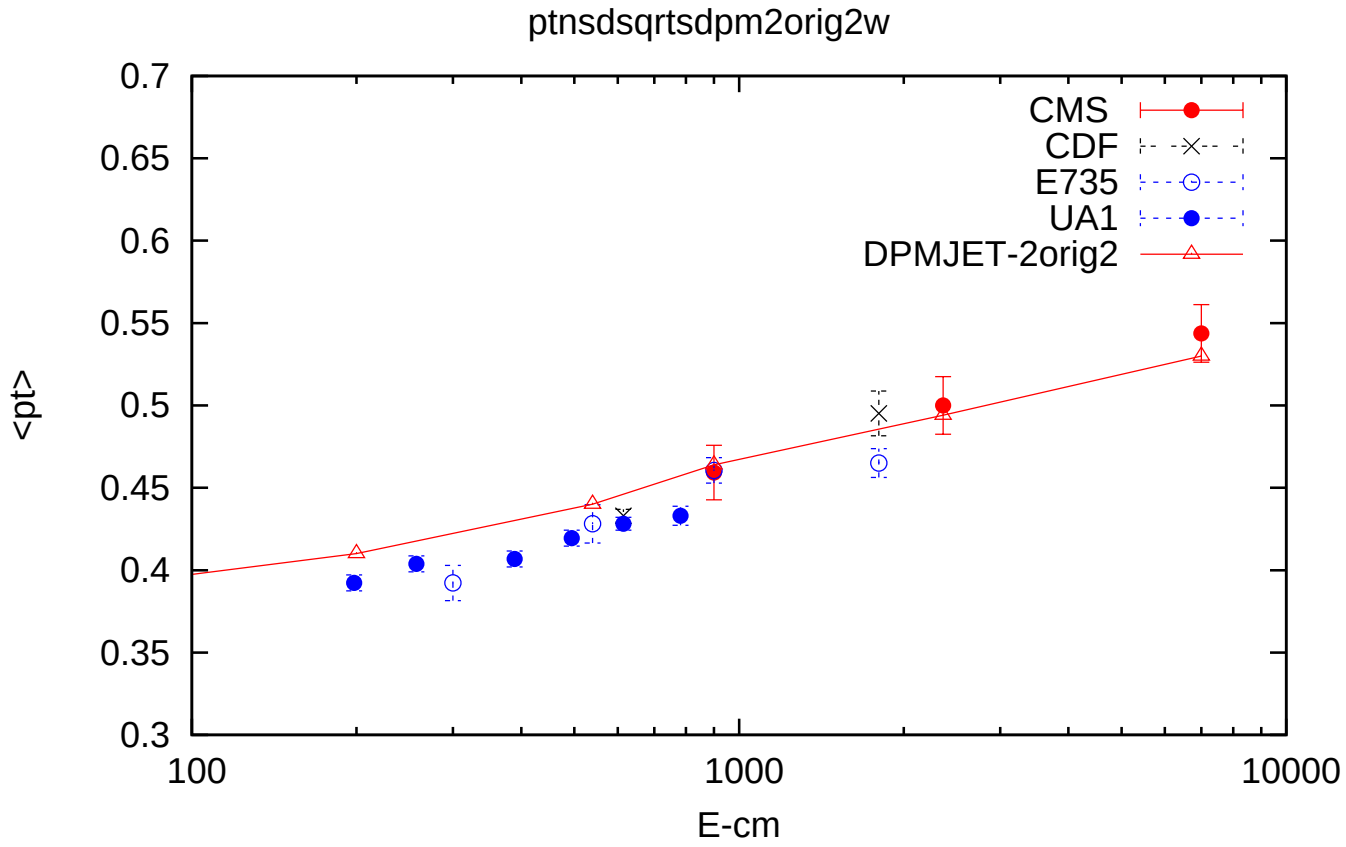
ptnsdsqrtsdpm2orig2w
CMS
CDF
E735
UA1
DPMJET-2orig2
<pt>
E-cm
0.7
0.65
0.6
0.55
0.5
0.45
0.4
0.35
0.3
100
1000
10000

This are the pt distributions at the 3 CMS energies

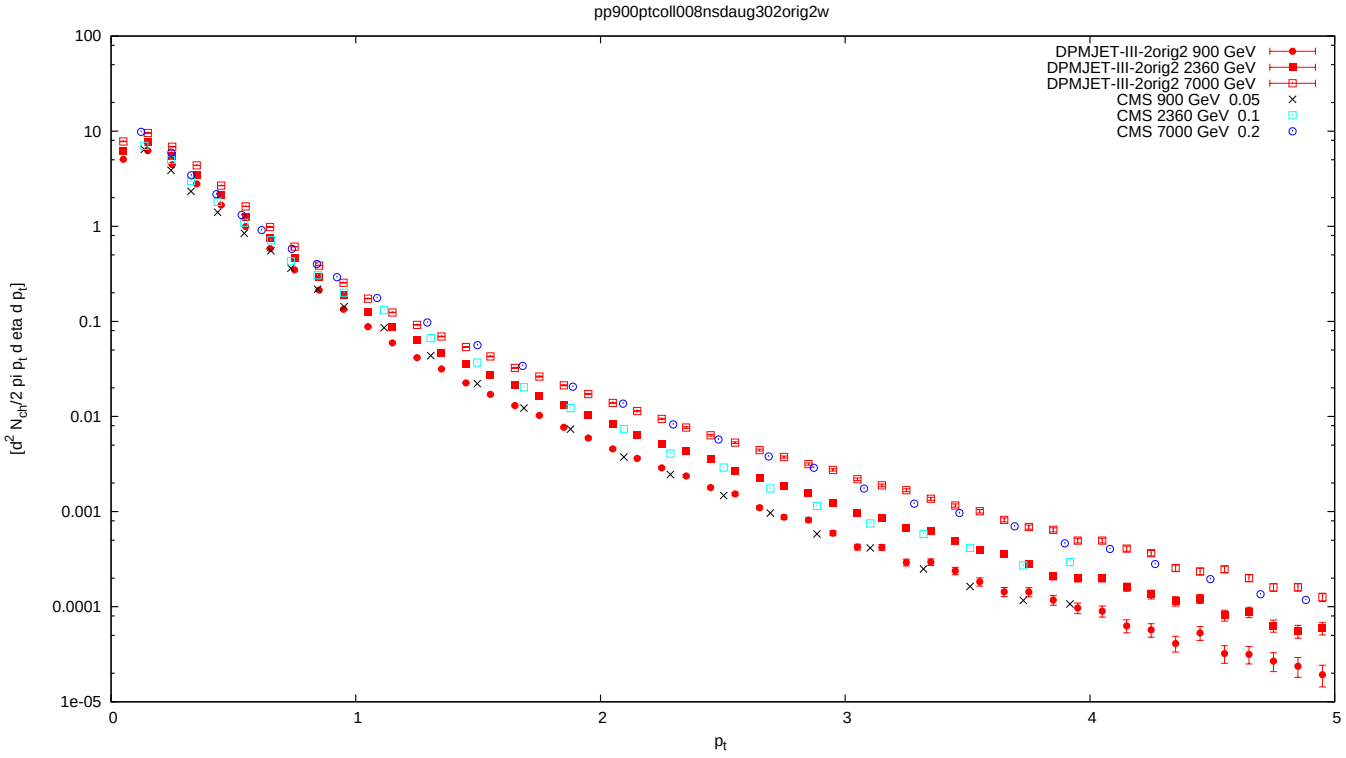

We come to the multiplicity distributions DPMJET compared to ALICE measurements

900 GeV

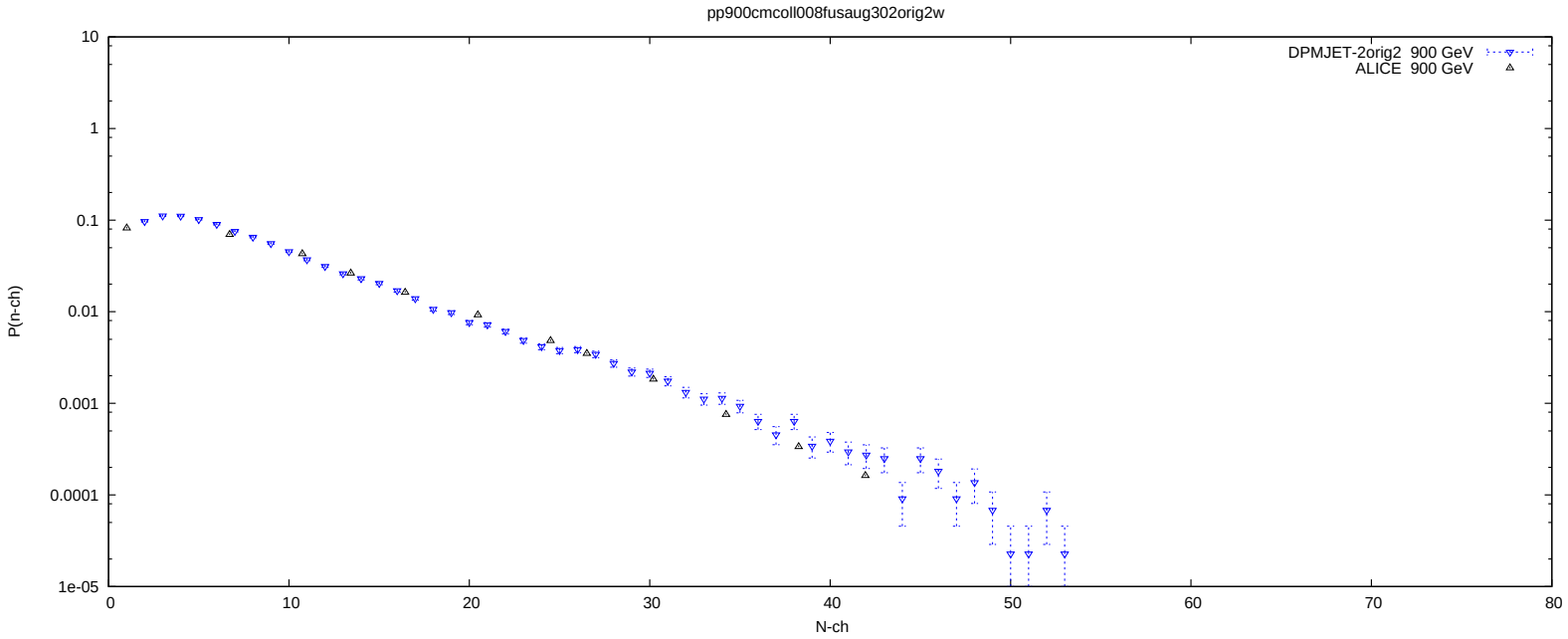

2360 GeV

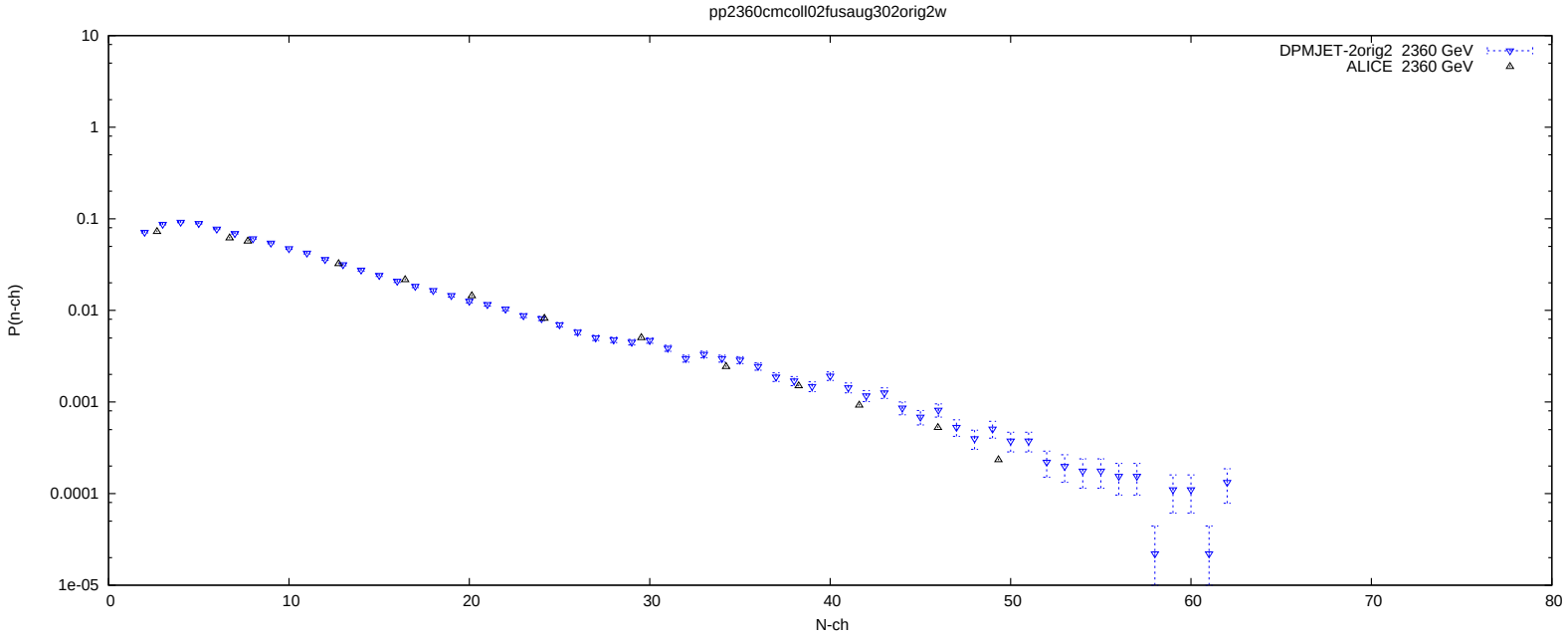
pp2360cmcoll02fusaug302orig2w
DPMJET-2orig2 2360 GeV
ALICE 2360 GeV
P(n-ch)
N-ch
10
1
0.1
0.01
0.001
0.0001
1e-05
0
10
20
30
40
50
60
70
80

7000 GeV

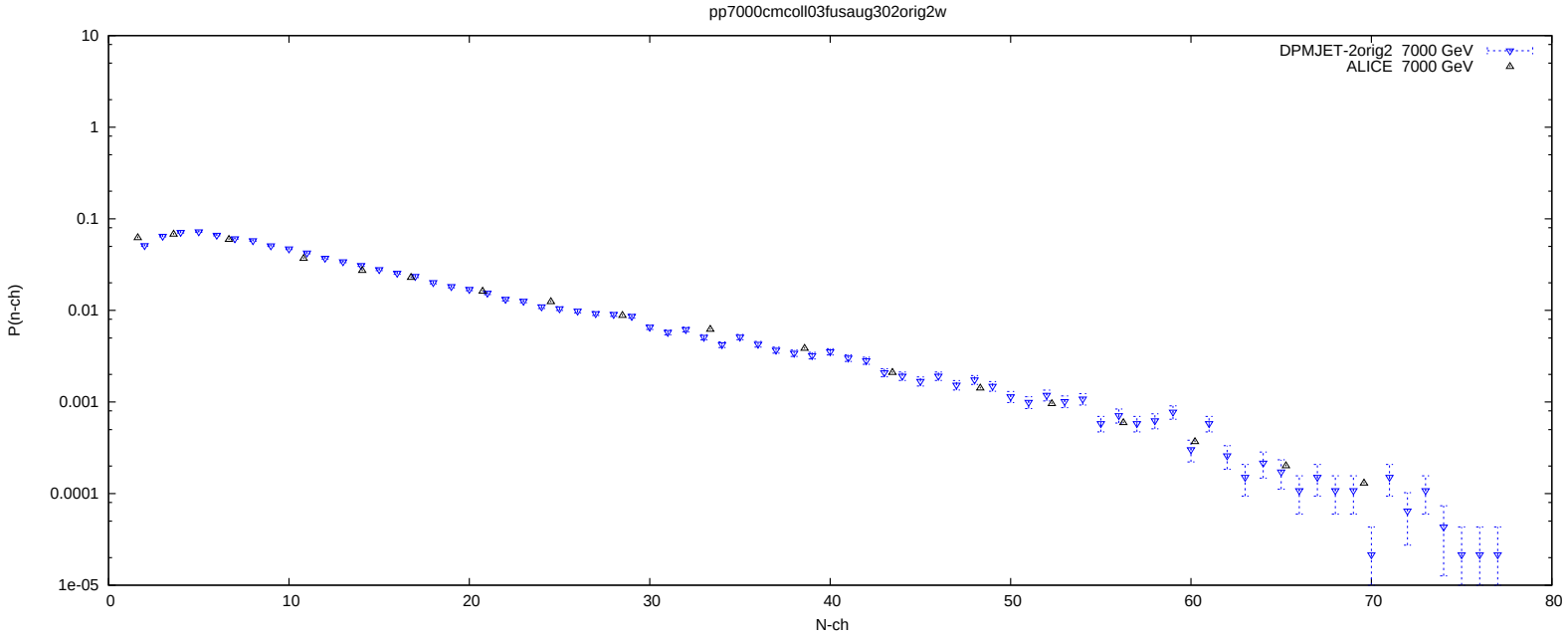
pp7000cmcoll03fusaug302orig2w
DPMJET-2orig2 7000 GeV
ALICE 7000 GeV
P(n-ch)
N-ch
10
1
0.1
0.01
0.001
0.0001
1e-05
0
10
20
30
40
50
60
70
80

Conclusion from LHC-data published so far:

The models (DPMJET-3, PHOJET, ...) agree very well with the LHC-data on particle production available so far

The p–p plateau values rise with energy faster than originally predicted by DPMJET-III.

This can be corrected by energy dependent parameters, but this solution can only be regarded as preliminary.

Let us hope, that new features on inclusive hadron production appear in forthcoming LHC-papers.

Let us hope to obtain soon data on hadron production in Pb-Pb collisions.